12

Flavor and transverse momentum generation and the vector meson to pseudoscalar meson ratio

12.1 Introduction

In this and the next chapter we are going to extend the Lund fragmentation model in several different directions in order to make it into a realistic model for the production of different kinds of hadron.

In the first section we start by investigating the classical motion of a string when it contains a $q\bar{q}$-pair having both mass and momentum components transverse to the string direction. One reason for doing this is to get an insight into the classical motion of a confined object. From this exercise we will learn that there are modes of motion of the massless relativistic string (the MRS) which contain much richer dynamics than that of a linearly rising potential. In this case the different parts (called 'segments') of the string will be found to move with respect to each other. We will meet similar examples later on in which our experience from this investigation will be useful.

It is possible to continue the investigation into the properties of the wave functions for this situation, [17]. Although we will present a few steps in that direction below a more complete treatment necessitates considerable mathematical machinery. The main result is, however, essentially the same as that obtained from the simple WKB-approximation, which was presented in Chapter 11.

The production of heavy quark masses and transverse momentum in a string field is intrinsically non-perturbative and leads to a gaussian suppression in both the quantities. The phenomena are governed by the string constant κ, i.e. the available energy per unit length along the force field. We will discuss a general process for transverse momentum generation and afterwards show its close resemblance to Brownian motion.

The results will necessitate a few phenomenological remarks. In particular it will become evident that heavy quark flavors like charm and

https://doi.org/10.1017/9781009401296.012 Published online by Cambridge University Press

bottom will never be produced during the fragmentation process of the Lund model. We briefly consider the pion-to-kaon ratio and its significance for measuring the strange-to-up and strange-to-down flavor ratios in multiparticle reactions.

We will after that consider the vector-to-pseudoscalar rate in a fragmentation process. The tunnelling process, which we deal with in the first section, also has implications for the relative rate of final-state hadrons. The produced $q\bar{q}$-particles have up to now been treated as if they were freely moving outwards after their production. This is evidently not the case in connection with the Lund model fragmentation process. In this process *they are tunnelling into bound-state hadronic wave functions.*

The classical turning point for the potential, i.e. the point where the kinetic energy vanishes for classical motion, is also the place where the virtual $q\bar{q}$-pair will come onto the mass shell after the production. The pair production rate is directly proportional to the squared wave function at this point. This is the place where the bound-state wave function starts to play a role for the produced q and $\bar{q}$. We will show that, depending upon the properties of the bound-state interaction, different kinds of hadron may have a different size of wave function at the turning point.

The spin-spin interaction between the constituents, which is different for vector mesons and pseudoscalar mesons, implies that the vector meson production rate should be suppressed compared with the pseudoscalar rate. In other words *it is more difficult to tunnel out into a vector meson state than into a pseudoscalar meson state.*

We consider a simple model for the phenomenon (a 'one-dimensional bag'). Then the relative rate behaves as a power law in the masses. The simplicity of the model prevents it from being a reliable tool for quantitative prediction of the suppression. But it provides a useful method of finding the wave functions for the tunnelling process, which we omitted before. We will also find qualitative agreement between the phenomenology and and the experimental observations.

We end by pointing out another problem, related to the production rate of η' particles. This also provides an opportunity to discuss the assignment of projection probabilities for the different flavor states in the Lund model.

12.2 The classical transverse motion of a string

The classical motion of a string when one of the endpoints has a momentum component transverse to the string direction is more complex than the modes of the MRS we have encountered up to now. The string field no longer behaves as a classical potential because different segments of the string are moving relative to each other.

https://doi.org/10.1017/9781009401296.012 Published online by Cambridge University Press

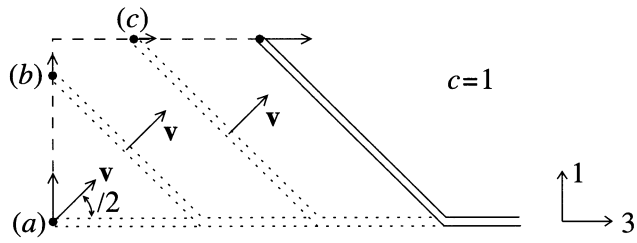

Fig. 12.1. The motion of a (massless) endpoint particle initially possessing transverse momentum together with the adjoining string piece. The times (*a*), (*b*) and (*c*) correspond to snapshots of the situation, as described in the text.

The transverse momentum of the endpoint is a very transitory property because of the interaction between the string and the particle at the endpoint, which will lead to a *transfer of the momentum from the endpoint particle to a region of the string in its neighborhood*. The size of this string segment is proportional to the size of the transverse momentum if the endpoint particle is massless and somewhat more complicated if the endpoint is a massive particle.

This means that transverse momentum is not a conserved property for such a particle, when it is part (and also generator) of a confining force field. But it is not possible to distiguish between the particle and the neighboring force field unless one introduces some measurement prescription.

We therefore feel confident in treating the particle quantum mechanically as an entity (although we are then also incorporating some part of the field in its neighbourhood). The major difference from the $(1+1)$-dimensional scenario we have discussed before is that a segment of the string containing transverse momentum will seem to have a larger longitudinal size, proportional to its transverse mass, rather than its ordinary mass.

1 *Transverse string motion with a massless endpoint particle*

Consider the situation depicted in Fig. 12.1(*a*) as a given starting point for the motion. The endpoint is assumed to have longitudinal momentum $k_3 = 0$ and a transverse momentum component $k_1 \neq 0$.

We assume that it is connected to a string stretched along the 3-direction, which is sufficiently long that we do not need to consider the other endpoint and its motion. We start with the case when the endpoint particle q is massless; we will discuss a set of snapshots of the motion in time.

https://doi.org/10.1017/9781009401296.012 Published online by Cambridge University Press

- After a time δt the endpoint has moved out along the 1-direction a distance δt ($c = 1$). A small region adjoining it has been affected (Fig. 12.1(b)). A signal has moved along the string also with the velocity of light so that the string segment between the endpoint and the rest of the string has a (geometrical) length equal to $\sqrt{2}\delta t$.

This segment is also in motion; it is evident that its velocity is

$$v = \frac{1}{\sqrt{2}} \tag{12.1}$$

This velocity, as in the transverse motion of the yoyo mode in Chapter 6, is related to the half angle $\theta/2$; in this case $\theta = \pi/2$:

$$\begin{aligned} v &= \cos(\theta/2) = 1/\sqrt{2} \\ \gamma(v) &= \frac{1}{\sqrt{1-v^2}} = \frac{1}{\sin(\theta/2)} = \sqrt{2} \end{aligned} \tag{12.2}$$

This means that the string segment will have the energy-momentum

$$\begin{aligned} e &= \kappa\sqrt{2}\delta t\,\gamma(v) = 2\kappa\delta t \\ p_1 &= \kappa\sqrt{2}\delta t\, v\gamma(v)\cos(\theta/2) = \kappa\delta t \\ p_3 &= \kappa\sqrt{2}\delta t\, v\gamma(v)\sin(\theta/2) = \kappa\delta t \end{aligned} \tag{12.3}$$

Consequently

- the endpoint has lost $\kappa\delta t$ both in energy and in the 1-component of its momentum, in accordance with the ordinary equations of motion. The string segment has picked up these quantities together with the energy-momentum which was in the string behind the moving signal-corner.

In this way we make use of the same considerations of local energy-momentum conservation as in Chapter 6 when we traced the transverse motion of the yoyo-state.

- This part of the motion continues until the endpoint q has lost all its original energy-momentum along the 1-direction. At that time it will start to move in the 3-direction (Fig. 12.1(c)). From now on, until the q reaches the other endpoint *the string segment serves only as a convenient transporter of energy-momentum to the endpoint q*. Thus the q-particle will gain energy-momentum along the 3-axis just as if it were a particle joined to an elastic cord, i.e. to the MRS.

In fact the string segment now picks up energy-momentum at the other end (from the remaining string), at the rate of κ per unit time and length, and delivers the same amount to the q. The string segment is in this

https://doi.org/10.1017/9781009401296.012 Published online by Cambridge University Press

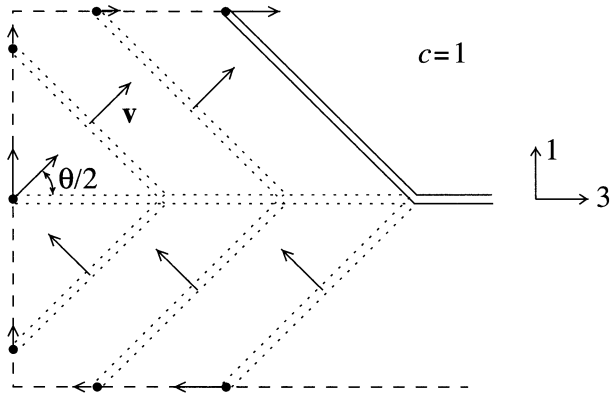

Fig. 12.2. The full motion when a q-particle comes in and leaves again. The q and the adjoining string segments share the transverse momentum in different proportions at different times.

way also moving on just like a rigid pole (but without changing its total energy-momentum).

In Fig. 12.2 we exhibit the full motion of a q-particle which comes in, dragging out the string behind it, and then turns around and leaves outwards again in accordance with the discussion above.

This corresponds to the motion discussed in Chapter 6, when a classical particle comes in and rebounds from the classical turning point. It is useful to trace the part of the motion before that discussed above, i.e. the motion inwards; we will leave it to the reader to understand the details by making use of local energy-momentum conservation and the fact that the endpoint particle moves with the velocity of light.

2 *Transverse string motion with a massive endpoint particle*

Before we display the above motion in a space-time diagram we will briefly consider the changes which occur when a massive q-particle (mass μ) is at the endpoint. The starting situation is the same as before but this time the endpoint is no longer moving with the velocity of light and consequently it can no longer go straight out along the 1-axis.

It will instead follow a hyperbola and, using the parameter $a(t)$ indicated in Fig. 12.3, we can write out the energy-momentum conservation equations. We use the indices p for the particle and s for the segment connecting the particle to the rest of the string. Let us suppose that the starting value of the particle's energy is $E_\perp = \sqrt{k_1^2 + \mu^2}$. Then the

https://doi.org/10.1017/9781009401296.012 Published online by Cambridge University Press

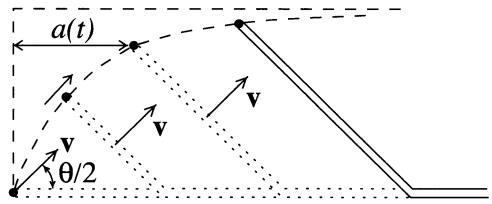

Fig. 12.3. The motion of a massive particle connected to a string when the particle initially possesses only a transverse momentum component.

equations for the conservation of energy and momentum will be

$$\begin{aligned} e_s(t) + e_p(t) &= E_\perp + \kappa t, \quad & e_s(t) &= 2\kappa(t-a) \\ p_{3s} + p_{3p} &= \kappa t, & p_{3s} &= \kappa(t-a) \\ p_{1s} + p_{1p} &= k_1, & p_{1s} &= \kappa(t-a) \end{aligned} \tag{12.4}$$

in accordance with the results in Eq. (12.3). We have used the fact that a string segment of a given size and with the transverse velocity given in Eq. (12.1) will have the same relation between size and energy-momentum as in the massless case. The string segment does not know that it is connected to a massive particle this time!

The requirement that the endpoint particle should be on the mass shell, i.e. $e_p^2 - p_{3p}^2 - p_{1p}^2 = \mu^2$, provides equations for the quantity $a = a(t)$ and also for the hyperbola along which the particle will move,

$$(\kappa x_{1p} - E_\perp)(\kappa x_{3p} + E_\perp - k_1) = -E_\perp(E_\perp - k_1) \tag{12.5}$$

(the coordinates x_{1p}, x_{3p} being defined with respect to an origin at the turning point). Note that when $\mu = 0$ we obtain the orbits shown above in Fig. 12.2. We leave it to the reader to prove Eq. (12.5) and to obtain the equation for $a(t)$.

In this way it is obvious that as long as we are not resolving the motion on a scale corresponding to the value of $\kappa(t - a(t)) - k_1$, i.e. $E_\perp - k_1$ (valid at large values of t) we do not know whether there is a massless or massive particle at the endpoint.

This is shown in a projection onto the tx_3-plane (i.e. the plane where the remainder of the string is dwelling) of the motion of a massless and of a massive endpoint particle (Fig. 12.4). We note in particular that the distances of closest approach (to the vertex of the hyperbola) in the two cases are given by $k_\perp = k_1$ and $E_\perp > k_1$ respectively.

https://doi.org/10.1017/9781009401296.012 Published online by Cambridge University Press

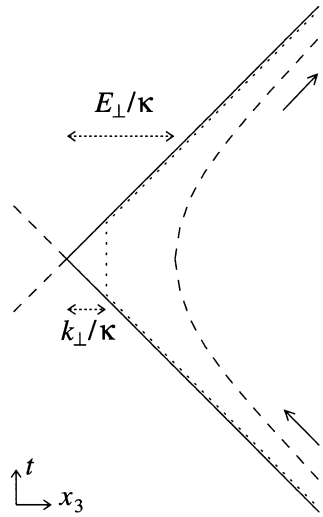

Fig. 12.4. The space-time diagram of the motion of an endpoint particle with a transverse momentum at the endpoint of a string, projected onto the plane spanned by the time and logitudinal direction of the string. The dotted line shows a massless particle; at closest approach it is at a distance $k_\perp/\kappa$ from the hyperbola focus. The broken line shows a massive particle; at closest approach it is at a distance $E_\perp/\kappa$ from the focus.

12.3 A general process for transverse momentum generation

1 Preliminaries

With the same methods used to derive the longitudinal fragmentation function we will now exhibit a general method for endowing the produced particles with transverse momentum. This leads to a correlation length in the model (further discussed and determined in Chapter 18). We will relate the result via the Langevin equation to Brownian motion; this is the Ornstein-Uhlenbeck process, [109].

We will assume that there is a set of hadrons produced along the positive lightcone direction; hadron j possesses transverse momentum $\mathbf{p}_j$. After n steps the total transverse momentum is $\mathbf{k}$:

$$\sum_1^n \mathbf{p}_j = \mathbf{k} \tag{12.6}$$

We now take one more step and produce a hadron with transverse mo-

https://doi.org/10.1017/9781009401296.012 Published online by Cambridge University Press

mentum $\mathbf{p}$, thereby reaching the next vertex with transverse momentum

$$\mathbf{k}' = \mathbf{k} + \mathbf{p} \tag{12.7}$$

We further assume the following.

- After many steps the distribution in $\mathbf{k}$, $f(\mathbf{k})d^2k$, 'saturates' and becomes independent of the earlier steps and there is no longer a preferred transverse direction.

- The transverse momentum production of the next hadron then only depends upon the the value reached, $\mathbf{k}$, and on the step, $\mathbf{p}$. We will in particular assume that *there is an anticorrelation* so that it depends upon the distribution $g(\mathbf{p}+\gamma\mathbf{k})d^2p$, γ being a positive number determined by what hadron is produced.

We may evidently also consider the vector $\mathbf{k}'$ as the result of the production of a set of hadrons along the negative lightcone with transverse momenta $\mathbf{l}_j$, thereby reaching the point

$$\mathbf{k}' = -\sum_{j=n+1}^{N} \mathbf{l}_j \tag{12.8}$$

(the minus sign is necessary to conserve the total transverse momentum, cf. Eq. (12.7) and we assume that there are N particles produced). The probability of doing this is again given by the saturating distribution $f(\mathbf{k}')d^2k'$. The next step from $\mathbf{k}'$ to $\mathbf{k}$, with $\mathbf{k} = \mathbf{k}' - \mathbf{p}$, thereby producing the hadron with transverse momentum $\mathbf{p}$, is given by $g(-\mathbf{p} + \gamma\mathbf{k}')d^2p$.

2 *The resulting distributions*

If we equate the two probabilities for producing a hadron with transverse momentum $\mathbf{p}$ we obtain (exchanging $\mathbf{p}$ for $\mathbf{k}' - \mathbf{k}$):

$$f(\mathbf{k})g(\mathbf{k}' + (\gamma - 1)\mathbf{k})d^2kd^2k' = f(\mathbf{k}')g(\mathbf{k} + (\gamma - 1)\mathbf{k}')d^2kd^2k' \tag{12.9}$$

After removing the differentials we may take logarithms of the functions (putting $\log f = F$, $\log g = G$) and then partial differentials of the result with respect to the same components of $\mathbf{k}$ and $\mathbf{k}'$. We note the similarity to the methods used in Chapter 8 to derive the longitudinal fragmentation function. Once again one set of functions vanishes, this time the f's.

We are then as in that case left with a second-order differential equation:

$$(\gamma - 1)\ddot{G}(\mathbf{k}' + (\gamma - 1)\mathbf{k}) = (\gamma - 1)\ddot{G}(\mathbf{k} + (\gamma - 1)\mathbf{k}') \tag{12.10}$$

https://doi.org/10.1017/9781009401296.012 Published online by Cambridge University Press

Therefore if $\gamma \neq 0, 1$ we conclude that the two sides must be equal to the same constant, to be called $-4\beta/[\gamma(2-\gamma)]$. We obtain directly the result

$$G(\mathbf{P}) = \log N - \frac{4\beta \mathbf{P}^2}{\gamma(2-\gamma)} \quad \rightarrow \quad g(\mathbf{P}) = N \exp\left[-\frac{4\beta \mathbf{P}^2}{\gamma(2-\gamma)}\right] \tag{12.11}$$

We have here invoked (euclidean) invariance, i.e. the assumption that there is no preferred direction. Therefore there is no linear term in the vector arguments.

The result for $F(f)$ is obtained by noting that if we introduce the result for $G(g)$ in Eq. (12.9) we may gather up the contributions depending upon $\mathbf{k}$ and $\mathbf{k}'$ on each side. The two sides must therefore again be equal to the same constant, $\log N'$:

$$F(\mathbf{P}) = \log N' - 4\beta \mathbf{P}^2 \quad \rightarrow \quad f(\mathbf{P}) = N' \exp(-4\beta \mathbf{P}^2) \tag{12.12}$$

The constants N, N' are evidently normalisation constants, while β, γ are dynamical quantities.

The result can be written in different ways. One interesting way is to write it as a squared matrix element (defining $\gamma \equiv 1 - \exp(-\tau)$):

$$f(\mathbf{k}) g(\mathbf{k}' - \exp(-\tau)\mathbf{k}) = |\mathscr{M}|^2, \quad \mathscr{M} = \langle 0 | \mathbf{k}' \rangle \, p_\tau(\mathbf{k}', \mathbf{k}) \, \langle \mathbf{k} | 0 \rangle \tag{12.13}$$

We have introduced the harmonic oscillator ground states (Chapter 3) in the momentum representation:

$$\langle \mathbf{k} | 0 \rangle = C \exp\left(-\beta \mathbf{k}^2\right) \tag{12.14}$$

The symmetrical function $p_\tau(\mathbf{k}', \mathbf{k})$ is equal to the *transition matrix* from the state $\mathbf{k}$ to the state $\mathbf{k}'$, cf. [83] and Eq. (12.24) below:

$$p_\tau(\mathbf{k}', \mathbf{k}) = \langle \mathbf{k}' | \exp(-H\tau) | \mathbf{k} \rangle \tag{12.15}$$

with H the harmonic oscillator hamiltonian in terms of the canonically conjugate variables $\mathbf{k}, \mathbf{b}$:

$$H = \frac{\sqrt{\beta}\mathbf{k}^2}{2} + \frac{\mathbf{b}^2}{2\sqrt{\beta}} \tag{12.16}$$

This brings out the symmetry of the results with respect to the transverse momentum and the impact parameter, $\mathbf{b}$. At the same time we note the similarity to Feynman's path-integral formulation of quantum mechanics, although the result refers to an imaginary time τ. The imaginary-time formalism fits into a statistical physics scenario and we will now show the close relationship between the results above and the velocity distribution of a particle undergoing Brownian motion.

It is of interest to note that motion in spacelike directions (i.e. in impact-parameter space) is formally equivalent to an imaginary-time formalism.

https://doi.org/10.1017/9781009401296.012 Published online by Cambridge University Press

This is evident from the considerations of Chapter 2, i.e. in spacelike directions the proper time τ becomes $i\sqrt{\mathbf{b}^2 - t^2}$.

3 The relation to Brownian motion: the Ornstein-Uhlenbeck process

Another way to understand the results in Eqs. (12.11) and (12.12) is to consider a seemingly different problem, the motion of a Brownian particle, mass m, under the influence of a friction force proportional to the velocity, $-m\rho v$, and a *gaussian random force*, mR. This is expressed by the Langevin equation:

$$\frac{dv}{dt} = -\rho v + R \tag{12.17}$$

In this way v is obtained as a *stochastical variable* defined by R. We assume that there is an ensemble of states on which measurements may be made. The ensemble average of a measurement of a dynamical variable a will be denoted $\langle a \rangle$.

We may evidently write as a general solution for Eq. (12.17):

$$v(t) = v(t_0)\exp(-\rho(t - t_0)) + \int_{t_0}^{t} dt' R(t')\exp(-\rho(t - t')) \tag{12.18}$$

The gaussian randomness assumption on R means that only 'white' noise is included. This means that R has a vanishing average value and only contains equal-time correlations; with I_R a constant we have for the ensemble averages

$$\begin{aligned} \langle R(t) \rangle &= 0 \\ \langle R(t)R(t') \rangle &= 2\pi I_R \delta(t - t') \end{aligned} \tag{12.19}$$

From this we conclude that the mean value and the *time correlation function* of v are given by

$$\begin{aligned} \langle v(t) \rangle &= \langle v(t_0) \rangle \exp[-\rho(t - t_0] \\ \langle v(t)v(t') \rangle &= \frac{\pi I_R}{\rho} \exp(-\rho|t - t'|) \end{aligned} \tag{12.20}$$

We have then assumed that the distribution is 'thermalised' at the starting time t_0 so that, according to the Maxwell velocity distribution,

$$\left\langle v^2(t_0) \right\rangle = \frac{\pi I_R}{\rho} = \frac{kT}{m} \equiv \frac{1}{2\beta} \tag{12.21}$$

It is then also the same for all times, $\left\langle v^2(t_0) \right\rangle \equiv \left\langle v^2(t) \right\rangle$, but there is an exponentially falling correlation between the value of v obtained at one time and at another. The correlation function depends only upon the

https://doi.org/10.1017/9781009401296.012 Published online by Cambridge University Press

time difference and therefore the stochastic process is called a *stationary stochastic process*. The variance of $v(t)$ is

$$\left\langle (v(t) - \langle v(t)\rangle)^2 \right\rangle = \frac{[1 - \exp(-2\rho(t - t_0)]}{2\beta} \tag{12.22}$$

If we define $u(t) = v(t) - \langle v(t)\rangle$ then $u(t)$ considered as a stochastical variable will have the particular *gaussian property that all higher-order correlation functions are determined by the two-point correlations*:

$$\left\langle \prod_{j=1}^{2n} u(t_n) \right\rangle = \sum_{perm} \prod_{j \neq k} \langle u(t_j) u(t_k)\rangle \tag{12.23}$$

i.e. they only contain all possible two-point correlations in time (the notation '*perm*' means all possible permutations of $1, \ldots, 2n$). The expectation value of an odd number of u's vanishes.

It is no coincidence that the Wick rearrangements of a time-ordered product of free fields, as discussed in Chapter 3, lead to the same results. The vacuum expectation values of free fields are just like the gaussian processes we consider here and the Feynman propagator corresponds to the correlations between two space time points.

The *transition probability* $P(v_0, t_0|v, t)$ from the value v_0 at t_0 to v at t is then given by the gaussian distribution

$$P(v_0, t_0|v, t) = \left\{ \frac{\beta}{\pi[1 - \exp(-2\rho\delta t)]} \right\}^{d/2} \exp\left\{ -\frac{\beta[v - v_0 \exp(-\rho\delta t)]^2}{1 - \exp(-2\rho\delta t)} \right\}$$

$$\int d^d v_1 P(v_0, t_0|v_1, t_1) P(v_1, t_1|v_1, t_1) = P(v_0, t_0|v, t), \quad t_0 \leq t_1 \leq t \tag{12.24}$$

Here we have introduced the number of dimensions, d, in which the process goes on and written $\delta t = t - t_0$ for the time difference.

It is not difficult to recognise the distribution g (with $\gamma = 1 - \exp(-\rho\delta t) \equiv 1 - \exp(-\tau)$) in the transition probability for the change in velocity of a Brownian particle in thermal equilibrium under the influence of gaussian white noise; see Eq. (12.11).

4 *Concluding remarks*

The formulation of transverse momentum generation above may seem abstract. It is obvious, however, that it corresponds to the possibility of producing a pair at every vertex with transverse momenta $\pm\mathbf{k}$. Together the q (with transverse momentum $-\mathbf{k}$) and the $\bar{q}$ (with $\mathbf{k}'$) from adjacent vertices will then combine to give a hadron with transverse momentum $\mathbf{p} = \mathbf{k}' - \mathbf{k}$.

https://doi.org/10.1017/9781009401296.012 Published online by Cambridge University Press

From this interpretation we may, using the tunnelling arguments in Chapter 11, identify the scale parameter, β, in terms of the string tension κ (note that the factor 4 in the definition of β in Eq. (12.11) is justified if we compare with the tunnelling process in Eq. (11.5) and also with the transition matrix elements in Eqs. (12.13) and (12.16)):

$$\beta = \frac{\pi}{4\kappa} \tag{12.25}$$

In the present Lund model the possibility of a correlation between the vertices for transverse momentum generation is not used, i.e. we have always put $\gamma = 1$. This corresponds to a large 'friction' coefficient, i.e. the 'memory' is very short.

There is, however, one kind of hadron, the pions, which have very small mass and for which, therefore, the two production vertices are very close. There are several indications that a proper treatment of the pions directly produced along the string actually does require a correlation, which then will diminish the transverse momentum of the final hadron. Note that the inclusive distribution of the hadron $\mathbf{p}$ is

$$\int d^2k f(\mathbf{k}) g(\mathbf{p} + \gamma\mathbf{k}) \quad \propto \quad \exp\left(-\frac{2\beta\mathbf{p}^2}{\gamma}\right) \tag{12.26}$$

This means that the mean transverse momentum of the hadron is

$$\sqrt{\langle \mathbf{p}^2 \rangle} = \sqrt{\frac{2\gamma\kappa}{\pi}} \tag{12.27}$$

which diminishes with γ. We will return to these features in Chapter 18.

12.4 The phenomenological implications of the tunnelling process

1 *The production of heavy flavors*

The results derived above are compatible with the WKB results, i.e. they are equivalent to Schwinger's result for the decay of the no-particle vacuum in the presence of an external electric field. We obtain for the $q\bar{q}$ production rate, with μ the mass and $\pm\mathbf{k}_\perp$ the transverse momenta of the pair,

$$dP \simeq d^2k_\perp \exp(-\pi E_\perp^2/\kappa), \quad E_\perp^2 = \mathbf{k}_\perp^2 + \mu^2 \tag{12.28}$$

The result in Eq. (12.28) has several different consequences.

The first is related to the relative abundance of different flavors in the fragmentation process. It is difficult to obtain precise mass-values for the unobservable $q\bar{q}$-particles but it is possible to obtain estimates.

https://doi.org/10.1017/9781009401296.012 Published online by Cambridge University Press

If we start with the heavy flavors, i.e. charm, c, and bottom, b, then there are potential models for the bound states of the $c\bar{c}$-states, J/Ψ and its relatives, and likewise for the corresponding $b\bar{b}$-states, Υ etc., [55].

These authors make use of nonrelativistic kinematics and potential terms containing Coulomb contributions, a linearly rising confining potential and also spin-spin and angular-momentum-spin interactions. In this way they obtain $\mu_c \sim 1.5$ GeV and $\mu_b \sim 5$ GeV (in both cases with a spread of a few hundred MeV).

Using the value $\kappa \simeq 0.2$ GeV^2 we find numbers smaller than 0.3×10^{-11} for the c-flavor production and vanishingly small numbers for the corresponding b-production. As the lighter-flavor masses are at most in the range of a few hundred MeV with small suppression we conclude that *c- and b-flavors are never produced in a fragmentation process.* The available energy density (κ) means that we need a string with a size at least around 3 fm to obtain a $c\bar{c}$-pair. At that point the lighter flavors have already supplied tremendous amounts of possible string-breakers.

2 *The production of light flavors*

The relative rates of u-, d- and s-flavor production are much more difficult to estimate. The reason is that there are different ways of attributing mass-values to these light flavors. In the classical treatment of the motion of a string with transverse momentum at the endpoint, we found that there is a certain region of the string close to the endpoint particle that exchanges energy-momentum with the particle. Thus it is difficult to distinguish between the particle and the field around it, at least in stable, long-time situations.

There is a corresponding notion in phenomenological models for the hadrons, i.e. the 'constituent quark mass' whereas in fast-production situations one talks of the 'current quark mass'. A quark-parton, which is exposed to an external probe acting very quickly in an almost pointlike way, is a current quark and one then expects to be able to neglect the field surrounding the quark charge. In the corresponding bound-state (stable) situation a constituent quark is always part of the bound-state force field and therefore 'heavier' than the 'bare' current quark.

If we compare the masses of the ρ-, K^*- and ϕ-mesons, which contain zero, one or two s- and/or $\bar{s}$-flavors, we may tentatively assign a mass difference $\mu_s - \mu_u \simeq 120$ MeV to the constituents. We are then referring the whole mass difference to the quark masses and are using a linear interpolation between the meson masses (there have been suggestions that the mass formulas should be quadratic for the mesons but we will not consider the reasons for such complications).

If we further assume that both the K^*- and the K-mesons are 'normal'

https://doi.org/10.1017/9781009401296.012 Published online by Cambridge University Press

with respect to chiral symmetry breaking (which strongly affects the mass of the π- and the ρ-mesons) then we could expect that the constituent u-quark mass is around 330 MeV. Then the ratio between the s- and the u-flavor rates should be close to 0.25 according to Eq. (12.28).

A change of κ to 0.24 GeV^{-2} or a reduction in the u-quark mass to 260 MeV will give a number close to 0.3. This seems to be the preferred relative fraction among the Monte Carlo users of the Lund model (i.e. the JETSET simulation program [105]), although 0.25 is not ruled out. In order to observe the ratio it is also necessary to take into account a few simple kinematical properties (cf. below in subsection 4).

3 *Transverse momentum generation*

We will later learn that the major contributor to the transverse momentum spectrum of the hadrons in high-energy interactions is the gluonic radiation. The transverse momentum we obtained in Eq. (12.27) should rather be looked upon as a quantum mechanical fluctuation in the ground state of the string (a zero-point fluctuation). These fluctuations imply that any primary meson should come out with a gaussian transverse momentum spectrum of width (the result stems from Eqs. (12.26) and (12.25))

$$\left\langle \mathbf{p}_\perp^2 \right\rangle = \frac{2\gamma\kappa}{\pi} \simeq (0.35)^2\gamma(\text{GeV}/c)^2 \tag{12.29}$$

We have inserted the word 'primary' above in order to distinguish between the hadrons that are produced directly in the fragmentation process and those which are actually observed. About half the primary particles are resonances and from the tables of the Particle Data Group one finds that they decay afterwards into many π's and K's. These decay products therefore constitute a large part of the observed charged particles.

The general preference of Monte Carlo users seems to be an average $\langle p_\perp \rangle \sim 0.4$ GeV/c, which is a little above Eq. (12.29) (with $\gamma = 1$). The difference can be easily attributed to soft gluonic radiation.

If we go back to the result in Eq. (12.28) then we may use the impact vector description from Chapter 10 to obtain an idea of the transverse width inside which the $q\bar{q}$-particles are produced. The matrix element becomes

$$\sim \int d^2p_\perp \exp\left(i\mathbf{p}_\perp\mathbf{b} - \frac{\pi\mathbf{p}_\perp^2}{2\kappa}\right) \simeq \exp\left(-\frac{\kappa\mathbf{b}^2}{2\pi}\right) \tag{12.30}$$

Thus the average impact-vector size is $\left\langle \mathbf{b}^2 \right\rangle = \pi/\kappa \simeq (0.8)^2\text{fm}^2$, a number almost twice as large as the transverse radius value we obtained from the phenomenology of the b-parameter in the Lund model in Chapter 11. However, we are not discussing the same quantity when we refer to the

https://doi.org/10.1017/9781009401296.012 Published online by Cambridge University Press

transverse size in connection with the b-parameter as when we refer to the size provided by the transverse momentum fluctuations in the string fragmentation process.

For the transverse momentum fluctuations it is not only the size of the string field but also the localisation of its centre which is of interest. Thus if we localise a quantum mechanical object very well in coordinate space then the wave function will evidently contain a large spread of momentum components in the dual space. The size 0.8 fm corresponds more to how well localised the string is in transverse directions than to the size of the emission region.

Note that the transverse momentum generation also influences the longitudinal distributions because in this case we must use the transverse mass $m_\perp = \sqrt{\mathbf{p}_\perp^2 + m^2}$ instead of the ordinary mass m. The reason is the relation $p_+ p_- = m_\perp^2$, which implies that we can conserve energy-momentum in the string plane only by this exchange.

4 *The mother-daughter relation*

There is another aspect of the resonance decays. The π's and K's from the decays populate phase space in different ways. There is a well-known kinematical property, usually referred to as the 'mother-daughter relation'.

Consider a resonance decay in the rest frame of the resonance. Obviously the decay products will go out in different directions in order to conserve the momentum. Their velocities are given by the mass of the particles, $\sqrt{1 - 4m^2/M^2}$ (cf. Chapter 4) when a resonance with mass M decays into two particles with the same mass m. This translates into a rapidity difference of the order of 1 to 2 units. (For $\rho \to \pi\pi$ decay, which is an extreme case because of the smallness of the π mass, one obtains, after angular averaging, around 1.5 units.)

Therefore the 'daughters', i.e. the decay products, tend to have roughly the same rapidity as the 'mother' so that they will have momenta which are proportional to their masses. In the decay of a K^* to a $K\pi$ this means that the (much) lighter π-particle in general takes a much smaller share of the mother's momentum than the K-particle. The π's also occur much more often as decay products than do other particles. The large amount of π's and the smaller correlation to their 'heritage' means that the π's occur in a rather uncorrelated fashion in the final states. They often have small momenta, in particular transverse to the jet.

This means that the central parts of rapidity space and the small transverse momentum region contains many more π's than K's and the ratio K/π is much smaller than the s/u ratio discussed above (typically below 0.1). If we consider the ratio K/π as a function of transverse

https://doi.org/10.1017/9781009401296.012 Published online by Cambridge University Press

momentum then it grows quickly with transverse momentum size and reaches for $p_\perp \simeq 0.4$ GeV (which corresponds to the average transverse momentum) the value 0.3.

We note, however, that if a primary π is produced with a large transverse momentum then there is a smaller difference from the production of a directly produced K because they will then have similar transverse masses.

12.5 Vector meson suppression

1 Preliminary remarks

At first sight one may guess that the ratio of the vector mesons (in the $J^{PC} = 1^{--}$ nonet; we use the usual notation with J the spin, P the parity and C the charge conjugation quantum number, cf. the Particle Data Group tables) to the pseudoscalar mesons (in the $J^{PC} = 0^{-+}$ nonet) should be 3 : 1. This is a purely statistical result corresponding to the number of states (three spin states for a vector as compared to the single spin 0 state for a pseudoscalar). The numbers of isospin and strangeness states are of course the same because the vector mesons and the pseudoscalars are both nonets in SU(3)-flavor.

This ratio is not in accordance with the results of e^+e^- annihilation experiments. Although it is difficult to disentangle the vector mesons (there are many possible combinations of K's and, particularly, of π's in a multiparticle final state) the general consensus for the PEP–PETRA energy region (20–40 GeV) is that the ratio of vector mesons to pseudoscalar mesons is in fact about 1 : 1 or maybe even smaller.

There is a good dynamical reason for this disagreement and we will now consider it in some detail. The vector meson wave functions are actually more difficult to tunnel into because they are smaller at the point, the classical turning point, where the produced q and $\bar{q}$ start to notice their final fate. The ensuing model should be applicable to all relative yields in which two produced hadrons, with similar quantum numbers, for some reason, e.g. due to constituent interactions, have different masses.

The q- and $\bar{q}$-particle stem from two adjacent vertices and there is an attractive force from the string which will bind them together. There are also, however, spin-dependent forces which will act in opposite ways in a pseudoscalar state and a vector state. The spin-spin correlation between particles 1 and 2 is positive for vectors and negative for pseudoscalars (note that the eigenvalue of $\mathbf{S}^2$ is $s(s+1)$):

$$\mathbf{S}_1 \cdot \mathbf{S}_2 = \tfrac{1}{2}\left[(\mathbf{S}_1 + \mathbf{S}_2)^2 - \mathbf{S}_1^2 - \mathbf{S}_2^2)\right] = \begin{cases} \tfrac{1}{4} & \text{for vectors} \\ -\tfrac{3}{4} & \text{for pseudoscalars} \end{cases} \tag{12.31}$$

https://doi.org/10.1017/9781009401296.012 Published online by Cambridge University Press

It is a very general property that all physical systems try to 'economise' with the energy. This means that in a system with a hamiltonian H (H_0 provides the space structure of the $q\bar{q}$ interaction),

$$H = H_0 + g\mathbf{S}_1 \cdot \mathbf{S}_2 \tag{12.32}$$

the constituents of a vector meson will try to avoid regions with positive g-values because the interaction energy of the state is increased in these regions and avoidance therefore implies a total decrease in the state energy. In contrast, for the pseudoscalar states it is advantageous for the constituents to be in regions with positive g-values. Therefore *we expect that the wave functions of the pseudoscalars will be concentrated in regions with g positive while the vector states will behave in the opposite way.*

This type of spin-dependent force occurs in a state with color-force binding, because of gluon exchange. It turns out that the effect has a very short-range character in coordinate space. A simple model for it is a positive contact form, which is very large when the constituents are close and vanishing when they are apart (x_j, $j = 1, 2$ are the coordinates of the particles and $\alpha > 0$ the effective coupling):

$$\alpha\delta(x_1 - x_2)\mathbf{S}_1 \cdot \mathbf{S}_2 \tag{12.33}$$

For such an interaction it is evident that in one space dimension the vector state, where the q- and the $\bar{q}$-particle try to stay apart, will be larger in size than the corresponding pseudoscalar state, where they would like to stay close together. A more spread-out vector meson wave function, which is still normalised to unity over the region, will be smaller at the classical turning point.

For real, three-space dimensional, bag models of the hadrons there is a corresponding effect, although the bag radii in this case are similar. Nevertheless the constituents in a vector meson bag move close to the outskirts of the bag so that they stay apart as much as possible while the pseudoscalar bag constituents tend to stay close together at the centre.

2 *A one-dimensional bag model*

We will now estimate the ratio, mentioned at the beginning of the last subsection by solving for the eigenstates of the hamiltonian in Eq. (12.32). For simplicity we will use nonrelativistic kinematics for H_0 (with equal masses μ for the q_1 and the $\bar{q}_2$):

$$H_0 = 2\mu + \frac{p_1^2}{2\mu} + \frac{p_2^2}{2\mu} + \kappa|x_1 - x_2| \equiv 2\mu + \frac{P_{cms}^2}{4\mu} + \frac{p^2}{\mu_r} + \kappa|x - x_0| \tag{12.34}$$

Here the cms motion of the pair has been omitted and we choose for the cms momentum eigenvalue $P_{cms} = 0$. The relative coordinates $x - x_0$ and

https://doi.org/10.1017/9781009401296.012 Published online by Cambridge University Press

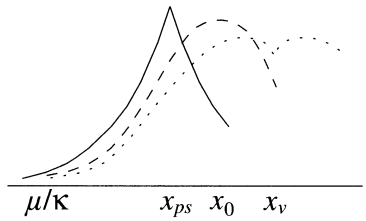

Fig. 12.5. The shapes of the wave functions corresponding to tunnelling into a vector meson (dotted line) and into a pseudoscalar meson (solid line) as well as into the Airy function ψ (broken line) mentioned in the text.

momentum p are introduced together with the reduced mass $\mu_r = \mu/2$. We will now construct the wave functions for the ground states in the pseudoscalar case, the vector case and the case when $\alpha = 0$ in Eq. (12.33), denoted $j = ps, v, 0$, respectively.

The linear potential evidently vanishes at $x = x_0$ and we note that for $x < x_0$ we have the differential equation

$$\left[-\frac{1}{2\mu_r}\frac{d^2}{dx^2} + \kappa(x_0 - x)\right]\Phi_j(x) = (E_j - 2\mu)\Phi_j(x) \tag{12.35}$$

For all wave functions Φ_j we choose a value of $x_0 \equiv x_j$ such that the left-most classical turning point (classically defined by $p = 0$ and quantum mechanically by an inflection point in the wave function) is at the same point $x = \mu/\kappa$. This means that for all cases when $x < x_j$ we have

$$\left(-\frac{1}{2\mu_r}\frac{d^2}{dx^2} - \kappa x\right)\Phi_j(x) = -\mu\Phi_j(x), \quad x_j = \frac{E_j - \mu}{\kappa} \tag{12.36}$$

This means that the wave functions for all j have the same behaviour in this region. The differential equation can be solved and one obtains a function, known as an Airy function (which we denote $\psi(x)$). It decreases exponentially along the negative x-axis. We do not need its properties but it is shown in Fig. 12.5.

The different wave functions do not need to be normalised in the same way and we therefore introduce the normalisation constants N_j:

$$\Phi_j(x) = N_j\psi(x), \quad x < x_j \tag{12.37}$$

From the symmetry of the problem we deduce that

$$\Phi_j(x) = N_j\psi(2x_j - x), \quad x > x_j \tag{12.38}$$

thus ensuing continuity at $x = x_j$.

https://doi.org/10.1017/9781009401296.012 Published online by Cambridge University Press

For the case when the spin-spin interaction vanishes ($j = 0$) the eigenvalue $E_0 = \kappa x_0 + \mu$ is determined from the requirement that the first derivative at $x = x_0$ should be continuous, which implies

$$\frac{\Phi_0}{dx}(x \equiv x_0) = \frac{d\psi}{dx}(x_0) = 0 \tag{12.39}$$

For the two other cases we obtain a discontinuous first derivative by integrating the differential equation over the region including the point x_j:

$$\lim_{\epsilon \to 0} \frac{1}{2\mu} \left[\frac{d\Phi_j}{dx}(x_j + \epsilon) - \frac{d\Phi_j}{dx}(x_j - \epsilon) \right] = \alpha \mathbf{S}_1 \cdot \mathbf{S}_2 \Phi_j(x_j) \tag{12.40}$$

This means

$$-\psi'(x_j)/[\mu\psi(x_j)] = \begin{cases} -3\alpha/4 & \text{for } j = ps \\ \alpha/4 & \text{for } j = v \end{cases} \tag{12.41}$$

We conclude that for the pseudoscalar (vector) case the ratio of the wave function and its derivative (known as the logarithmic derivative) is positive (negative) while for the case $j = 0$ it vanishes.

The function ψ starts out very small, for large negative x-values, and then increases towards a maximum at the value $x = x_0$; afterwards it decreases. Therefore we conclude that the value $x = x_{ps}$ must be on the upward slope, and the value $x = x_v$ on the downward slope, in order that the logarithmic derivatives should have the right signs.

Thus we obtain without much effort that

$$x_{ps} < x_0 < x_v \tag{12.42}$$

which is basically what we set out to prove, namely that the vector meson state in this one-space dimensional model is essentially larger than the pseudoscalar state in extension.

It is also rather easy to estimate the relative size of the wave functions at the classical turning point, because this is given by

$$\frac{|\Psi_v|^2}{|\Psi_{ps}|^2} = \frac{|N_v|^2}{|N_{ps}|^2} \tag{12.43}$$

i.e. by the normalisation condition for the integrals

$$1 = |N_j|^2 \left(\int_{-\infty}^{x_j} dx |\psi(x)|^2 + \int_{x_j}^{\infty} dx |\psi(2x_j - x)|^2 \right) \tag{12.44}$$

As the functions are subject to exponential rapid decrease outside the classical turning points and vary reasonably slowly in between these points we can estimate that the ratio in Eq. (12.43) is

$$\frac{|N_v|^2}{|N_{ps}|^2} \simeq \frac{x_{ps}}{x_v} = \frac{E_{ps} - \mu}{E_v - \mu} \tag{12.45}$$

https://doi.org/10.1017/9781009401296.012 Published online by Cambridge University Press

A more detailed numerical investigation of the ratio tells us that Eq. (12.45) is a very good approximation if the ratio is larger than $\simeq 0.2$. For smaller values of $E_{ps} - \mu$ the ratio in the first line of Eq. (12.45) levels out and for a vanishing $E_{ps} - \mu$ the ratio of the normalisation constants becomes $\simeq 0.12$. The question whether there should be one factor for the q and another for the $\bar{q}$ is probably of little interest because of the general simplicity of the model.

Phenomenologically the Lund model has been successful with the following suppression rates:

$$\frac{\rho}{\rho + \pi} \simeq 0.5, \quad \frac{K^*}{K^* + K} \simeq 0.6, \quad \frac{D^*}{D^* + D} \simeq 0.75 \tag{12.46}$$

We note that there is a clear tendency that the closer the masses of the vectors and the pseudoscalars, the closer we come to the statistical value 3 : 1.

3 *The η' puzzle*

In order to exhibit the way in which the Lund model distributes the probabilities for different flavor configurations and also to mention a current phenomenological problem we will discuss the assignment of probabilities to the isoscalar states η and η'. Recently some doubt has appeared, [51], about the $\rho/(\rho + \pi)$ ratio – it should probably be even smaller than we predicted in the earlier section, maybe in the range 0.3–0.4. It turns out, however, that the η' has a large branching ratio for the decay

$$\eta' \to \rho + \pi \tag{12.47}$$

and in this way the number of η'-particles will influence the observed ρ-signal. We will now show that according to the Lund model rules the number of η'-particles must be enhanced if we suppress the directly produced ρ-particles. But then we will get back a large ρ-rate through the decay channel in Eq. (12.47). To get around the problem diminishing the ρ-rate we must therefore also suppress η'. The practical effect is then that we give an overall enhancement to the π-mesons!

According to the philosophy of the model all states should be populated according to the probability of projecting out a given flavor composition upon them. The η and η' in the pseudoscalar nonet (from now on called PS) play the same role as the ϕ and the ω for the vector (V) mesons.

In more detail, a state with the third component of isospin vanishing is, in $SU(3)_f$ (with f for flavor) either the $I_3 = 0$ component, ($|0_j\rangle$), of the isovector (ρ_0 for the V and π_0 for the PS) or the total singlet state ($|1_j\rangle$) or octet state ($|8_j\rangle$) in either nonet; $j = PS, V$. Knowing that

https://doi.org/10.1017/9781009401296.012 Published online by Cambridge University Press

$|0_j\rangle = (|u\bar{u}\rangle - |d\bar{d}\rangle)/\sqrt{2}$ (compare with the spin 1 states built from spin 1/2!) we may write for the other states

$$|1_j\rangle = \frac{|u\bar{u}\rangle + |d\bar{d}\rangle + |s\bar{s}\rangle}{\sqrt{3}}, \quad |8_j\rangle = \frac{|u\bar{u}\rangle + |d\bar{d}\rangle - 2|s\bar{s}\rangle}{\sqrt{6}} \tag{12.48}$$

to obtain orthogonal combinations in the three flavors u, d, s. There is, however, one further degree of freedom, called 'mixing', meaning that the true observed states may be mixtures of the singlet and octet states:

$$\begin{aligned} |h_{j1}\rangle &= |8_j\rangle \cos\theta_j - |1_j\rangle \sin\theta_j \\ |h_{j2}\rangle &= |8_j\rangle \sin\theta_j + |1_j\rangle \cos\theta_j \end{aligned} \tag{12.49}$$

The vector nonet states are 'simple' from the point of view of mixing. The ϕ-particle is almost a pure $s\bar{s}$-state, as it decays almost exclusively into a $K\bar{K}$-pair. Therefore the V mixing angle $\theta_V \sim 0.62$ so that $\tan\theta_V \simeq 1/\sqrt{2}$. Then the ω-particle is the combination $(|d\bar{d}\rangle + |u\bar{u}\rangle)/\sqrt{2}$. But the pseudoscalar nonet states η and η' are more complex flavor states: different authors (cf. the Particle Data Group tables) assign different mixing angles θ_{PS} from -0.17 to -0.40.

Now suppose that we start with a u (or d) and pick up from the next vertex a $\bar{u}$ (or $\bar{d}$). Then we may produce either a vector state (ρ_0 or ω) or a pseudoscalar state (π_0, η or η') according to the assignments given above. If we suppress the vectors we enhance the pseudoscalars and therefore the decay channel in Eq. (12.47) will also be enhanced!

We will in Chapter 14 again find reasons for suppressing the η'-rate (which actually is not very well known from direct measurements). One possible clue to such a dynamical suppression is the very large masses of the η and η'. There have been different models suggested (mostly built upon the possibility that the vacuum exhibits a dynamical 'chiral symmetry breaking', which we will have no space to consider in this book).

In such models there will necessarily be some mechanism which makes the isoscalar states more massive than the corresponding isovector ones in the PS nonet. This will then, in all cases, have the further effect that we obtain a suppression factor similar to the one we found in our one-dimensional bag model, the spin interaction being exchanged for the mechanism that makes the isoscalars more massive.